molecules

MDPI

Review

Nanotechnology-Based Strategies for Safe and Effective Immunotherapy

Seeun Hong †, Juwon Park †, Yoojeong Oh †, Hanhee Cho and Kwangmeyung Kim *

Graduate School of Pharmaceutical Sciences, College of Pharmacy, Ewha Womans University, Seoul 03760, Republic of Korea; hongseeun@ewhain.net (S.H.); parkjoowon@ewhain.net (J.P.); ubellro@ewhain.net (Y.O.); ricky@ewha.ac.kr (H.C.)

* Correspondence: kimkm@ewha.ac.kr

† These authors contributed equally to this work.

Abstract: Cancer immunotherapy using immune checkpoint blockades has emerged as a promising therapeutic approach. However, immunotherapy faces challenges such as low response rates in solid tumors, necessitating strategies to remodel the immune-suppressive tumor microenvironment (TME) into an immune-activated state. One of the primary approaches to achieve this transformation is through the induction of immunogenic cell death (ICD). Herein, we discussed strategies to maximize ICD induction using nanoparticles. In particular, this review highlighted various studies integrating chemotherapy, radiation therapy (RT), photodynamic therapy (PDT), and photothermal therapy (PTT) with nanoparticle-based immunotherapy. The research covered in this review aims to provide valuable insights for future studies on nanoparticle-assisted immunotherapy.

Keywords: drug delivery; cancer treatment; nanoparticle; immunotherapy; chemotherapy; photodynamic therapy; photothermal therapy; radiotherapy

check for updates

Citation: Hong, S.; Park, J.; Oh, Y.; Cho, H.; Kim, K. Nanotechnology-Based Strategies for Safe and Effective Immunotherapy. *Molecules* **2024**, *29*, 5855. https://doi.org/10.3390/molecules29245855

Academic Editor: Adrian Keller

Received: 30 October 2024
Revised: 3 December 2024
Accepted: 10 December 2024
Published: 11 December 2024

Copyright: © 2024 by the authors. Licensee MDPI, Basel, Switzerland. This article is an open access article distributed under the terms and conditions of the Creative Commons Attribution (CC BY) license (https://creativecommons.org/licenses/by/4.0/).

1. Introduction

Cancer immunotherapy has gained significant attention as a revolutionary strategy in oncology for achieving the complete cure of cancer and has been broadly applied regardless of cancer type or stage [1–3]. The major difference between immunotherapy and conventional cancer treatments lies in the fact that immunotherapy activates the patient's own immune system to treat even cancers that cannot be treated through surgery or chemotherapy [4,5]. While traditional chemotherapy is limited by non-specific toxicity and the challenge of treating metastatic cancer due to the lack of selectivity and acquired resistance, immunotherapy can target not only the primary tumor but also metastatic sites through the activation of the adaptive immune response [6–9]. These treatments typically inhibit the function of immune checkpoint proteins such as programmed cell death protein 1 (PD-1), programmed cell death ligand 1 (PD-L1), and cytotoxic T-lymphocyte-associated protein 4 (CTLA-4), which play a key role in immune evasion [10–12]. By blocking, degrading, or suppressing the generation of these immune checkpoint proteins, immunotherapy allows cytotoxic T cells to recognize and eliminate tumor cells more effectively [13,14].

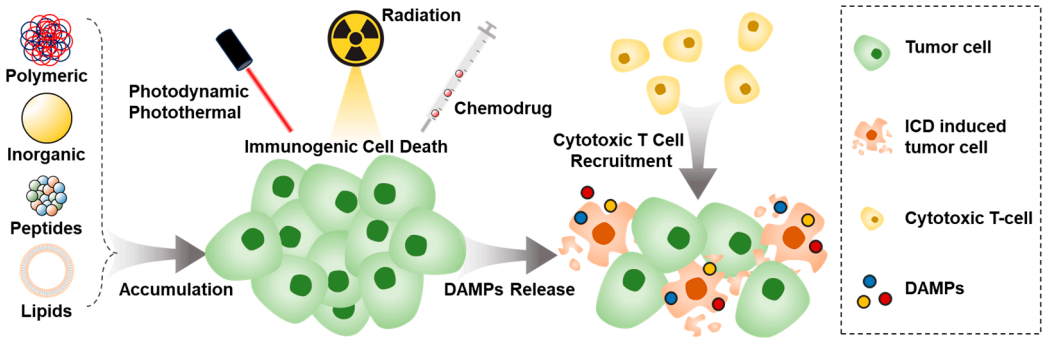
Despite this remarkable performance, immunotherapy still confronts many hurdles such as low patient response rates, high costs, and toxicity related to self-immunity [15,16]. Among these, the low response rate is a primary challenge that must be addressed, as it is a common issue in the majority of solid tumors [17,18]. Unlike hematological tumors, immune responses in solid tumors are mainly driven by antigen presentation through dendritic cells and macrophages [19–21]. However, the immunosuppressive TME induces the upregulation of regulatory T cells (Tregs), myeloid-derived suppressor cells (MDSCs), vascular endothelial growth factor (VEGF), and transforming growth factor β (TGF-β), leading to the M2 polarization of macrophages, which further promotes an immunosuppressive

state [22,23]. Therefore, remodeling the TME to create an immune-activated environment could serve as an effective approach to overcoming the low response rate [24,25].

Inducing ICD in tumor cells is one approach to remodeling the TME [24,26]. Well-known ICD inducers include anthracycline-based drugs like doxorubicin (DOX), as well as treatments such as PDT, RT, and PTT [27]. These treatments generate stress, such as DNA damage and reactive oxygen species (ROS) production, leading to ICD, which induces damage-associated molecular pattern (DAMP) signals [28,29]. DAMPs include immunogenic signals, such as high-mobility group box 1 (HMGB1), calreticulin (CRT), and adenosine triphosphate (ATP) [30]. Each signal plays a distinct role in activating immune responses. For instance, HMGB1 suppresses immunosuppressive components such as Tregs and MDSCs through the toll-like receptor 4 (TLR4) pathway, while enhancing immune-inflammatory responses within the tissue [31]. CRT, acting as an "eat-me" signal, is translocated to the cell surface via the eukaryotic initiation factor 2 α-activating transcription factor 4-C/EBP homologous protein (eIF2α-ATF4-CHOP) pathway, thereby promoting the polarization of macrophages toward the M1 phenotype [32,33]. ATP functions as a "find-me" signal, recruiting immune cells to sites of inflammation [34]. Through this cascade of events, dendritic cells are activated and matured, enabling the presentation of tumor antigens via both MHC class I and II pathways [35]. As a result, this can effectively resolve issues like low T lymphocyte infiltration caused by immunosuppressive conditions in tumors, enhancing the efficacy of immune checkpoint inhibitors (ICIs) in solid tumors [36,37].

However, the non-specific toxicity due to the low specificity and targeting efficiency of ICD inducers are significant challenges for combination treatment with ICIs [38,39]. The low specificity and lack of targeting efficiency prevent sufficient delivery of ICD inducers to tumor sites, hindering the effective induction of the ICD required for immune activation [40]. Furthermore, attempting to resolve this issue with high doses may lead to severe systemic side effects and non-specific toxicity to immune cells [39]. This could result in inadequate immune responses, even if ICD is induced, due to the depletion or dysfunction of immune cells. Thus, optimizing the dosage is crucial; therefore, the drug delivery system using nanoparticles such as peptides, proteins, polymeric, inorganic, dendrimers, or liposomes presents a promising approach to overcoming these challenges [41–48]. First, nanoparticles can enhance drug efficacy by taking advantage of the enhanced permeation and retention (EPR) effect, which leads to tumor accumulation due to the leaky blood vessels caused by tumor angiogenesis [49,50]. In addition to delivering drugs, the surface of nanoparticles can be easily modified with molecules, peptides, or proteins to target tumor-specific receptors, thereby improving targeting efficiency and providing additional synergistic effects with encapsulated drugs [51,52]. This strategy enables specific targeting of tumor tissue, which minimizes the non-specific toxicity of ICD inducers and immunotherapeutic agents resulting in the maximization of drug efficacy and, as a result, the reduction of the relative cost [53,54]. Moreover, it facilitates effective TME remodeling, helping to overcome immunosuppressive conditions and improving the overall immune response, which can help address the low response rates of currently used ICIs in clinical settings [55,56].

Herein, we propose the study of nanoparticles for remodeling the TME by introducing ICD-inducing treatments, such as chemotherapy, PDT, RT, and PTT (Scheme 1). These studies successfully remodeled the TME via inducing ICD, transforming the immunosuppressive condition into an immune-activated environment [57]. In addition to addressing methods for overcoming immunosuppressive conditions, we present future perspectives on nanoparticle-based immunotherapy, providing deep insights for future research into TME remodeling using nanoparticles.



Scheme 1. Schematic illustration of ICD-inducing mechanisms through chemotherapy, PDT, RT, and PTT utilizing nanoparticles. Several nanoparticles allow for the accumulation of encapsulated drugs in the tumor tissue, and induced ICD remodeled immune-suppressive TME to an immune-activated environment through the DAMP release resulting in enhanced T cell recruitment to the tumor tissue.

2. Chemotherapy with Nanoparticles for ICD

Chemotherapy is one of the most effective approaches for ICD [58,59]. Several chemotherapeutic agents, such as doxorubicin, mitoxantrone, and oxaliplatin, are known to induce ICD [60]. For instance, doxorubicin induces cell death by causing DNA damage and generating ROS, ultimately leading to apoptosis [61]. This process triggers sufficient endoplasmic reticulum (ER) stress through an intrinsic pathway and extrinsic pathway, finally activating the protein kinase RNA-like endoplasmic reticulum kinase (PERK)-eukaryotic initiation factor 2α (elF2α)-C/EBP homologous protein (CHOP) pathway for promoting cell apoptosis [62–64]. These processes effectively induce ICD; therefore, combining doxorubicin with immunotherapy can enhance the anti-tumor immune response and improve treatment efficacy [65–67].

Kim et al. developed a liposome-encapsulated prodrug composed of an inhibitor of apoptosis protein (IAP)-inhibiting peptides and DOX to enhance ICD through synergistic effect for maximizing the therapeutic effect of combination therapy with PD-L1 antibody (Figure 1A) [68]. They conjugated peptide sequences, including a second mitochondria-derived activator of caspase (SMAC) mimetic peptide (AVPIAQ) and cathepsin B cleavable peptide (FRRG), to doxorubicin, and then encapsulated in PEGylated liposomes (Aposome). The formulated liposomes were analyzed through dynamic light scattering (DLS) and transmission electron microscope (TEM) with an average size of 100 nm (Figure 1B). Aposome was only activated in tumor cells due to the cancer-overexpressed cathepsin B with no toxicity observed in normal cells and immune cells. Owing to the synergistic effects of SMAC and DOX, higher expression levels of DAMPs such as CRT, HMGB1, and ATP in Aposome-treated CT26 tumor cells were observed compared to DOX- and DOXIL-treated groups (Figure 1C). They also demonstrated the enhanced targeting efficiency of Aposome compared to DOX, due to the EPR effect induced by liposome formulation (Figure 1D). As a result, the Aposome group treated with a PD-L1 antibody showed improved tumor growth suppression with an 80% clearance rate (Figure 1E), and the upregulation of cytotoxic $CD8^+$ T cells was observed from excreted tumor tissues in Aposome groups treated with PD-L1 antibody (Figure 1F).

Yang and colleagues investigated paclitaxel (PTX)-induced ICD to improve the immune response of the PD-1 antibody [69]. They introduced methoxy-poly(ethylene glycol)-*b*-poly(D, L-lactide) (mPEG-PDLLA) to formulate PTX-encapsulated nano-micelle (Nano-PTX) for enhancing tumor-targeting efficiency and reducing non-specific toxicity. As expected, the Nano-PTX-treated group showed enhanced $CD8^+$ cytotoxic T cells in excised tumor tissue from CT26-bearing mice compared to the control group. They demonstrated the release of DAMPs in Nano-PTX-treated CT26 colon cancer cells such as CRT and HMGB1 as the reason for the enhancement of $CD8^+$ T cells, which results in the upregulation of phagocytosis and immune-active cytokines. Based on these results, the PD-1 antibody was co-administered with Nano-PTX in the MC38 mouse model, resulting in a

78% tumor clearance rate compared to the control group and monotherapy groups. Furthermore, when a rechallenge was performed on the models with tumor clearance, none of the mice exhibited tumor growth, which was presumed to be due to immune memory.

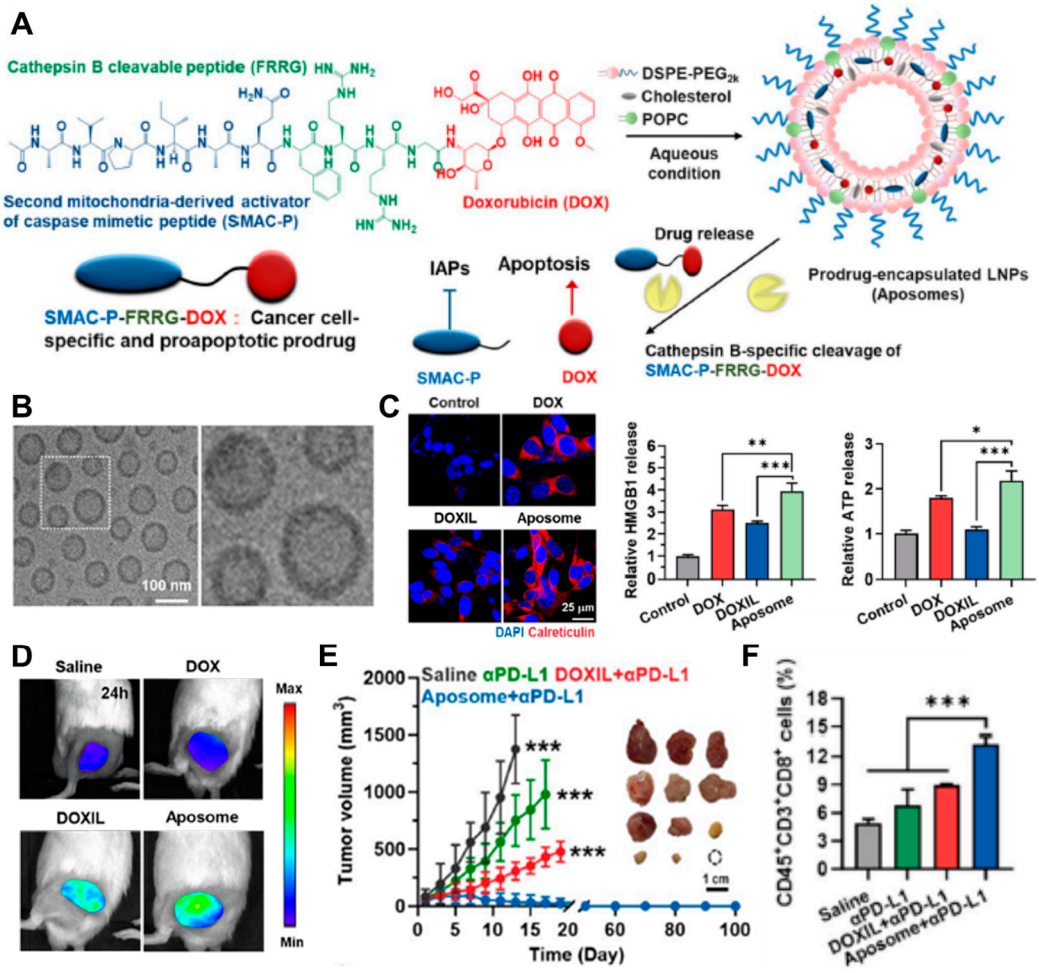


Figure 1. (**A**) Schematic illustration of the cancer-specific and proapoptotic prodrug SMAC-P-FRRG-DOX loaded into LNPs. (**B**) TEM images of Aposomes with a size of 100 nm. (**C**) The release of DAMPs (CRT, HMGB1, ATP) after DOX, DOXIL, or Aposome treatment. (**D**) In vivo fluorescence images after DOX, DOXIL, and Aposome treatment in the CT26 tumor xenograft model. (**E**) The tumor growth curve of the CT26 mouse model treated with saline, a PD-L1 antibody, DOXIL with a PD-L1 antibody, and Aposome with a PD-L1 antibody. (**F**) The relative $CD8^+$ T cell expression level in excised tumor tissue on day 13. Significance was determined by the Tukey−Kramer post hoc test (* $p < 0.05$, ** $p < 0.01$, *** $p < 0.001$). Reproduced with permission [68]. Copyright: BMC, 2024.

Zhang et al. developed DOX and PD-L1 blockade peptide P-12 (FPNWSLRPMNQM) encapsulated lipids/poly(lactic-co-glycolic acid)(PLGA) dual composition nanoparticles for ICD-induced immunotherapy [70]. They established the nanoparticle composition with optimal drug encapsulation and release profiles with a size of 100–125 nm, and finally optimized lipid/PLGA nanoparticles with 30% of DSPE-PEG_{5000} and 10% of cell penetration peptide R8-conjugated DSPE-PEG_{2000}. DOX and P-12 were encapsulated in optimized lipid/PLGA nanoparticles (LPN-30-$R8^{2k}$) and were efficiently absorbed into CT26 cells, inducing ICD and resulting in the upregulation of CRT as a DAMP. The LPN-30-$R8^{2k}$ effectively targeted the tumor tissue in a CT26-bearing mouse model via IV injection, due to the EPR effect of the nanoparticle formulation. As expected, enhanced tumor growth suppression was observed in the LPN-30-$R8^{2k}$-treated CT26 mouse model, and the upregulation of cytotoxic T lymphocytes and the downregulation of Tregs were analyzed

from excised tumor tissue compared to other groups due to enhanced DAMPs being released by encapsulated DOX.

Song and colleagues developed surface-modified chitosan nanoparticles (CNP) encapsulating chemotherapeutic agents [71]. They prepared CNP by introducing a PD-L1 peptide antagonist onto their surface (PP-CNP), which blocked the cancer immune checkpoint protein PD-L1 via a multivalent binding mechanism. Additionally, the CNPs encapsulated DOX as an ICD inducer and were delivered to the tumor site via the EPR effect. The synergistic effect of DOX and PD-L1 peptide blockade led to tumor clearance 60 days after the first subcutaneous inoculation of CT26 cancer cells in mouse flank accompanied by an activated immune response, including enhanced $CD8^+$ T cell and downregulated $CD25^+$ Tregs. Furthermore, DOX-loaded PP-CNP showed improved therapeutic efficacy in a lung metastasis model, enabling survival of the treated mice at the end of the treatment, whereas all of the other groups exhibited a zero-survival rate.

3. PDT with Nanoparticles for ICD

PDT is a treatment method that uses light-sensitive compounds called photosensitizers (PS) such as verteporfin, chlorin e6, zinc phthalocyanine, and aluminum phthalocyanine tetrasulfonate, which cause effective ICD for cancer immunotherapy [72,73]. When PS absorbs specific wavelengths of light, the energy level within the PS rises from the ground state to the excited state [74,75]. During the process of returning to the ground state, the PS interacts with surrounding molecules such as oxygen to generate various ROS through both type I and type II mechanisms [75–77]. Similarly to the mechanism of chemotherapy, the generated ROS induces cell death by triggering ER stress, leading to significant ICD [78,79]. As a result, DAMPs are secreted from apoptotic cells, allowing the immune system to recognize and attack tumor cells efficiently [80–82].

Choi et al. conjugated photosensitizer verteporfin (VPF) and indolamine 2,3-dioxygenase (IDO) degradable proteolysis targeting chimera (PROTAC) through tumor-overexpressed enzyme cathepsin B cleavable linker peptide (KRR) to form light-triggered PROTAC nanoassemblies (LPNs) (Figure 2A) [83]. The LPNs were 102.49 $\pm$ 7.39 nm in size with a spherical structure (Figure 2B); they maintained their size for 48 h. Due to the ROS generation via light irradiation to verteporfin in the LPNs, DAMP secretions such as HMGB1, ATP, and HSP70 were upregulated in CT26 tumor cells compared to the treatment without light (Figure 2C). Moreover, due to the spherical structure with an appropriate size for inducing the EPR effect, LNPs showed enhanced tumor-targeting efficiency in the CT26 tumor-bearing mouse model relative to the verteporfin-treated group (Figure 2D). The LPNs with light irradiation showed a 100% clearance rate (n = 5) (Figure 2E) resulting from improved $CD8^+$ T cell activity and impeded $CD25^+$ Tregs activity due to the induced ICD (Figure 2F). In addition, there was no tumor recurrence when CT26 tumor cells were inoculated into tumor clearance mouse species, and it is due to the adaptive immunity by $CD44+/CD62L^{low}$ memory T cell.

Wang et al. designed a PDT-immunotherapy system by utilizing membrane-coated nanoparticles (MON) to amplify antitumor immune responses through ROS generation [84]. They focused on spatially packaging antigen ovalbumin (OVA) for encapsulating photosensitizer Ce6 to construct an immunogenic and ICD-inducible nanoparticle. These nanoparticles were formulated by loading the photosensitizer Ce6 to OVA complex, coated with the membrane of B16-OVA cells. The nanoparticles showed a final size of approximately 85 nm, enabling effective tumor targeting. Upon laser irradiation, the ROS generated by Ce6-induced ICD released DAMPs such as CRT and HMGB1, which enhanced phagocytosis and cytokine production. In vivo experiments using B16-OVA tumor models demonstrated that MON treatment achieved complete tumor regression and prevented metastasis through an abscopal effect. Additionally, MON therapy promoted a strong immune response, with increased $CD8^+$ T cells and reduced Tregs, establishing immune memory that effectively prevented tumor recurrence upon rechallenging.

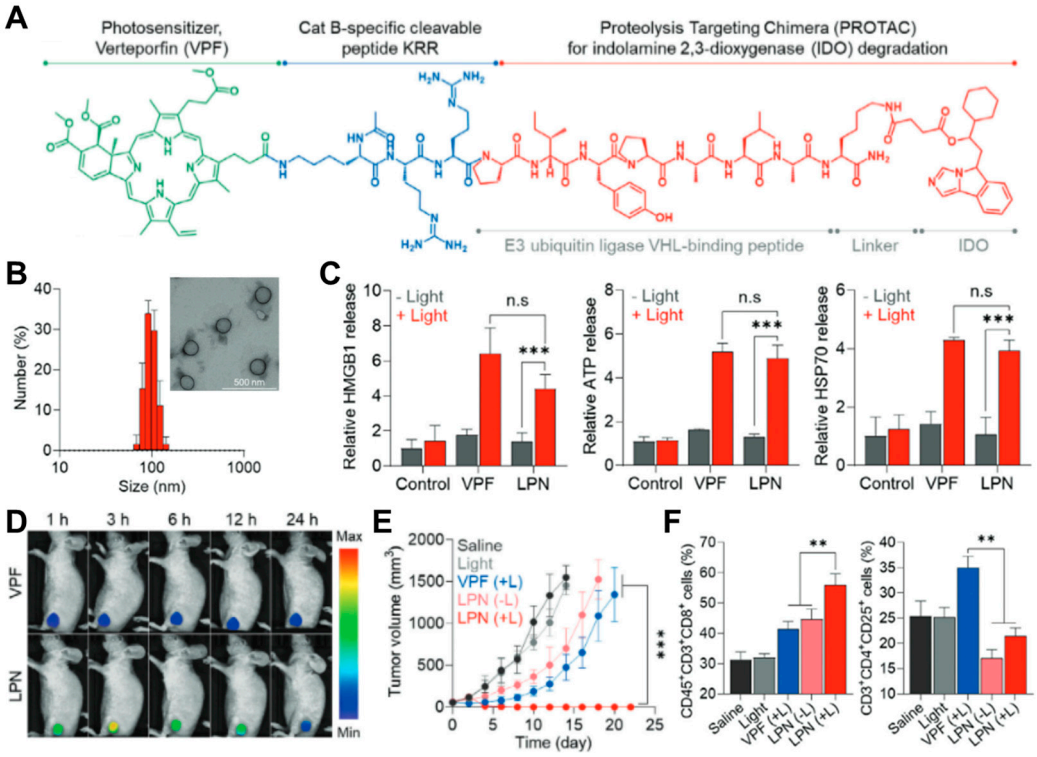


Figure 2. (**A**) Chemical structure of cathepsin-B activatable VPF-IDO PROTAC prodrug. (**B**) TEM images of LPNs with size of 102.49 ± 7.39 nm confirmed by DLS. (**C**) Relative DAMP expression level after treatment of VPF or LPN, with or without light irradiation. (**D**) Fluorescence images of CT26-bearing mouse model treated with VPF or LPN. (**E**) Tumor growth curve after treatment of light irradiation, VPF with light irradiation, and LPN with or without light irradiation. (**F**) Relative expression level of $CD8^+$ and $CD25^+$ cells in excised tumor tissue. Significance was determined by one-way ANOVA with Tukey–Kramer post hoc test (** $p < 0.01$, *** $p < 0.001$). Reproduced with permission [83]. Copyright: Wiley-VCH GmbH, 2024.

Zhao and colleagues investigated PDT combined with PTT using indocyanine green (ICG)-loaded nanoaggregates (ICG-DNA) to induce ICD and enhance systemic antitumor immunity [85]. The nanoparticles were formulated by coordinating ICG with a thermosensitive polymer, $p(MEO_2MA_{160}$-*co*-$OEGMA_{40})$-*b*-pSS_{30} (POEGS), resulting in an average particle size of 197 nm (TEM) and 246.8 nm (DLS). While 808 nm light irradiation, ICG-DNA produced singlet oxygen ($^1O_2$), triggering the release of DAMPs such as CRT and HMGB1, resulting in activated phagocytosis and promoting immune-active cytokine expression. In a bilateral 4T1 tumor model, treatment with ICG-DNA (P/I = 6.55) effectively eradicated primary tumors and exhibited an abscopal effect by inhibiting distant tumor growth. The enhanced immune response was evidenced by increased $CD8^+$ cytotoxic T cells and reduced Tregs, along with higher levels of mature dendritic cells (DCs), leading to a robust antitumor immune response and preventing tumor recurrence during the rechallenge test.

Jin et al. tried to address the limitations of traditional PDT, such as the low tissue penetration of visible light required for ROS generation and poor bioavailability, by utilizing lanthanide-doped upconversion nanoparticles (UCNPs) [86]. Additionally, they employed a click reaction to conjugate rose bengal (RB) and ROS-specific release-capable DOX onto UCNPs. The nanoparticles were then coated with cell membranes extracted from 4T1 cancer cells, providing immune evasion properties and enhancing tumor accumulation. Upon applying 980 nm NIR irradiation, which can penetrate deep tissues, the UCNPs emitted visible light luminescence, triggering ROS generation by the encapsulated RB. This effectively induced cell death within the tissue. Moreover, the ROS-triggered release of DOX

caused a synergistic ICD induction. In a lung metastasis animal model, the combination treatment with an antibody against CD73, which inhibits T cell infiltration, further amplified immune responses, including the upregulation of $CD8^+$ T cells and $CD86^+$ cells and the downregulation of Tregs. This approach resulted in a 93.4% reduction in tumor growth compared to the control group.

4. RT with Nanoparticles for ICD

RT is another strategy to induce ICD, transforming immunosuppressive TME into an immune-activated condition [87]. RT is a cancer treatment method that uses ionizing radiation to damage the DNA of tumor cells, leading to their destruction [88,89]. The ionizing radiation generates ROS and causes direct DNA double-strand breaks, resulting in severe cellular damage and apoptosis [90,91]. DNA damage and ROS-induced ER stress trigger cell death mechanisms similar to those previously mentioned, making RT capable of effectively inducing ICD [92–94]. Therefore, the combination of localized radiotherapy and immunotherapy could be utilized as an efficient immunotherapeutic strategy while minimizing side effects for patients [95–97].

For robust cancer immunotherapy, Chen et al. combined radiotherapy as a strong ICD-inducing strategy [98]. They developed PLGA nanoparticles which encapsulated water-soluble catalase (Cat) as an oxygen supplier and imiquimod (R837) as a toll-like receptor 7 agonist and triggered potent ICD through radiation exposure for enhanced treatment efficiency of CTLA-4 antibody (Figure 3A). The Cat and R837 containing PLGA nanoparticles (PLGA-R837@Cat) were observed via TEM and DLS, showing a homogeneous size of around 100 nm as spherical structures (Figure 3B). In addition, PLGA-R837@Cat-treated tumor tissue escaped from hypoxia condition compared to control and PLGA-R837-treated groups overcoming insufficient oxygen supply, which is one of the current challenges of radiotherapy. Also, due to the CRT expression found by X-ray irradiation (Figure 3C), primary tumors and secondary inoculated tumors with the PLGA-R837@Cat treatment combined with CTLA-4 antibody showed complete tumor regression (Figure 3D). As expected, improved $CD8^+$ cytotoxic T cells and suppressed Tregs in $CD4^+$ T cells were observed in PLGA-R837@Cat with CTLA-4 antibody-treated tumor tissues compared to other groups (Figure 3E).

Wang et al. developed oxaliplatin/Fe (OXA/Fe) bimetallic nanoparticles as cascade-sensitizing amplifiers to enhance low-dose radio-immunotherapy [99]. The size of nanoparticles was shown 106.6 nm with a spherical morphology, which was confirmed by DLS and TEM. These nanoparticles exhibited increased X-ray sensitivity through encapsulated Fe; thus, ROS generation was amplified, inducing strong ICD with enhanced CRT exposure and HMGB1 release as evidence. Intravenous injection of OXA/Fe NPs in a CT26 tumor xenograft model followed by low-dose X-ray irradiation resulted in the effective regression of both primary and abscopal tumors, with heightened CRT exposure in excised primary tumor and superior $CD8^+$ T cell activity in the abscopal tumors. This treatment not only promoted tumor regression but also established immune memory, preventing metastasis and recurrence.

The nanoscale coordination polymers composed of gadolinium, 5′-Guanosine monophosphate, and Hemin (H@Gd-NCPs) were developed by Huang et al. [100]. The efficacy of radiation was enhanced in two ways. First, the encapsulated gadolinium amplified X-ray absorption leading to effective immunogenic cell death. Second, Hemin exhibited peroxidase-mimetic activity, providing an H_2O_2 supply to overcome the hypoxic tumor microenvironment. As a result, the H@Gd-NCPs with 112.5 nm size showed enhanced tumor growth suppression in the CT26 xenograft model compared to other groups when combined with X-ray radiation. In addition, CRT and HMGB1 secretion were detected from excised tumor tissue, with the highest expression levels detected in the H@Gd-NCPs treated group following radiation. H@Gd-NCPs with radiation and an anti-PD-L1 antibody was further treated in the abscopal model, resulting in a significant increase in $CD8^+$ T cells

and interferon-γ (INF-γ) at both the primary and distant tumors, leading to 37.5% tumor clearance at the distant site.

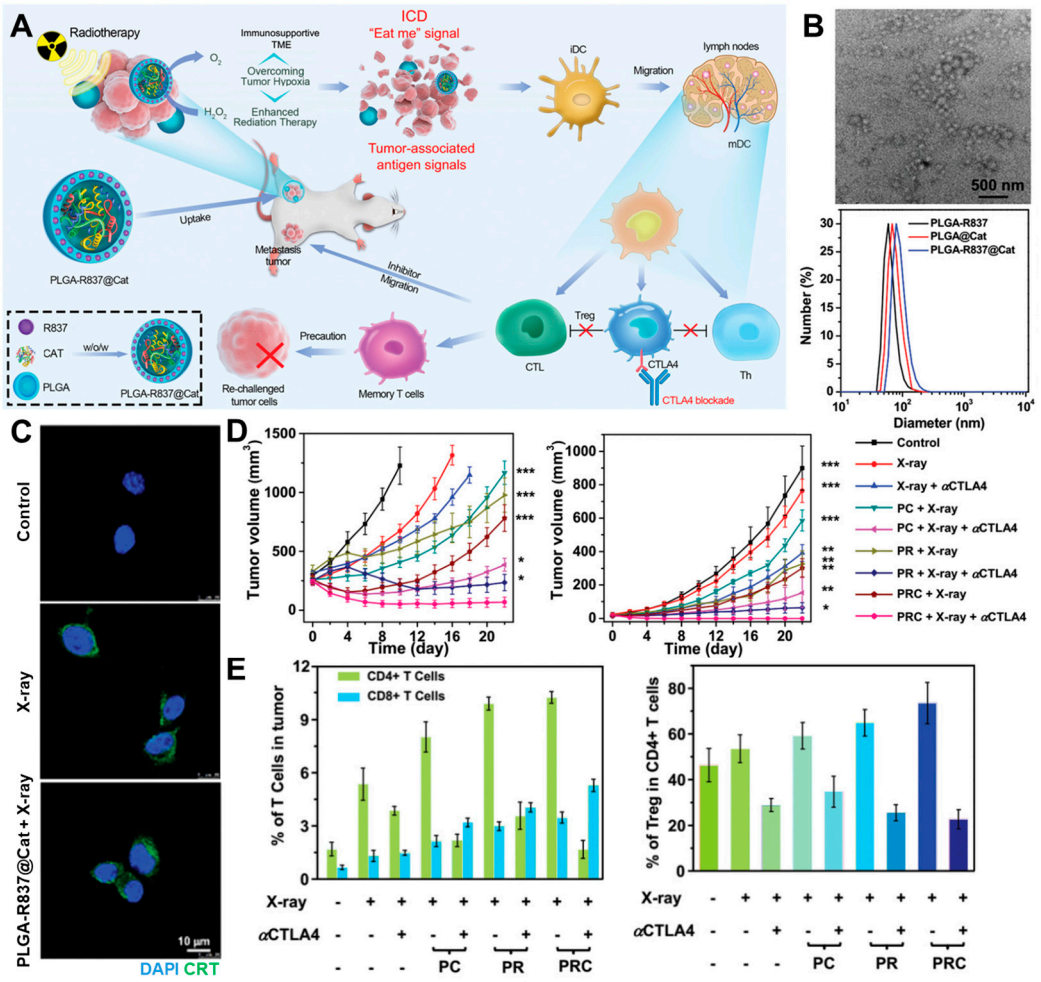


Figure 3. (**A**) Schematic illustration of PLGA-R837@Cat. (**B**) TEM images of PLGA-R837@Cat and DLS confirmation with a size of 100 nm. (**C**) Fluorescence images of CRT exposure after X-ray irradiation or PLGA-R837@Cat treatment with X-ray irradiation. (**D**) The growth curve of a primary tumor and a secondary inoculated tumor with various treatment conditions. (**E**) The relative expression level of T cells and Tregs at the excised tumor tissue. Significance was determined by one-way ANOVA using the Tukey post-test. (* $p < 0.05$, ** $p < 0.01$, *** $p < 0.001$). Reproduced with permission [98]. Copyright: Wiley-VCH GmbH, 2019.

Guan et al. developed a PEGylated hollow manganese dioxide (HMP)-based nanoplatform for enhanced post-surgical RT and immunotherapy [101]. The system combines the hypoxia-relieving properties of MnO_2, which decomposes tumor-derived H_2O_2 into oxygen, with the tumor-targeting delivery of a PI3Kγ inhibitor (IPI549) to reduce MDSCs and reprogram the TME. This approach improves RT efficacy by enhancing immunogenic cell death and sensitizes tumors to anti-PD-L1 therapy. In murine models of colon and melanoma cancer, the combination therapy significantly inhibited residual and metastatic tumor growth, induced strong immune memory, and achieved complete protection against tumor rechallenging in 100% of treated mice. The strategy demonstrates the potential of nanosystems for synergistic radioimmunotherapy and immune modulation.

5. PTT with Nanoparticles for ICD

PTT is another effective treatment for inducing ICD [102]. PTT utilizes nanoparticles or other heat-sensitive agents such as gold nanoparticles, graphene oxide, and car-

bon nanotubes, and these agents generate localized heat upon exposure to near-infrared light [103–106]. Electron clouds in these materials are excited by absorbed light, and this phenomenon is known as plasmon resonance [107]. After excitation, the energy level of the electron cloud decreases to the ground state, with energy transfer inducing moderate heating in the range of 41 to 47 °C [108–110]. The heat from energy transfer causes selective tumor eradication due to its poor blood supply compared to normal tissue [111]. This heat-induced cell death also triggers the release of DAMPs, leading to immune cell activation through induced ICD [112,113]. As a result, combining PTT with immunotherapy can amplify the anti-tumor immune response and improve the overall treatment outcomes [102,114,115].

Tang et al. developed gold nanorods (AR) and CRISPR/Cas9 to induce ICD through the photothermal effect and disrupt PD-L1 for achieving effective immunotherapy [116]. They fabricated double-coated cationic gold nanorods (ANP) using polystyrene sulfonate (PSS) and polyethyleneimine-modified β-cyclodextrin with biguanidyl adamantane (PCM), enabling the intracellular delivery of a CRISPR/Cas9 plasmid with a heat-inducible promoter (HSP-Cas9) (Figure 4A). The HSP-Cas9 activated the transcription of Cas9 and its associated sgRNA upon exposure to mild hyperthermia, then silencing PD-L1 at a genomic level. The structure of the synthesized AR was observed by TEM, revealing a rod structure with a length of 60.14 nm and a width of 8.02 nm (Figure 4B). Moreover, the photothermal effect, generated by the gold nanostructure upon light irradiation-induced ICD, is evidenced by the release of HMGB1 and the exposure of CRT and HSP70 in B16F10 cancer cells (Figure 4C). As expected, the group treated with ANP/HSP-Cas9 (ANP/P) and light irradiation exhibited the most effective tumor regression, attributed to both ICD and PD-L1 disruption caused by the plasmid (Figure 4D). This result was confirmed by a reduced Treg ratio and an increased M1/M2 ratio in the excised tumor (Figure 4E).

Meanwhile, Li et al. conducted a study on a dual immunotherapy model combining PTT and PDT [79]. They developed ER-targeting pardaxin (FAL) peptides and indocyanine green (ICG) conjugated hollow gold nanospheres (FAL-ICG-HAuNS). Additionally, they designed hemoglobin liposomes conjugated with FAL (FAL-Hb-lipo) to overcome hypoxic conditions. The sizes of FAL-ICG-HAuNS and FAL-Hb-lipo were 151 ± 4.6 nm and 160.5 ± 6.6 nm, respectively. Due to rapid cellular internalization and high stability facilitated by FAL, both particles exhibited strong tumor accumulation and retention. The combination therapy of FAL-ICG-HAuNS and FAL-Hb-lipo maximized tumor growth suppression following laser irradiation, attributed to the high tumor-targeting ability, PDT effect of ICG, PTT effect of HAuNS, and oxygen delivery by Hb. These outcomes were further validated by the exposure of CRT in the tumor, which led to immune cell activation such as $CD8^+$ T cells and the upregulation of immune cytokines such as INF- γ and IL-6.

Chen et al. developed nanoparticles by templating manganese dioxide (MnO_2) with bovine serum albumin (BSA) and conjugating it with the anticancer drug DOX (DOX-BSA/MnO_2) [117]. The developed DOX-BSA/MnO_2 nanoparticles formed spherical structures with a size of 32.5 ± 2.31 nm, which enabled higher tumor-targeting efficiency compared to free drugs. Additionally, when DOX-BSA/MnO_2 combined with laser irradiation was applied to 4T1 cells, the results demonstrated effective ICD induction, as evidenced by increased CRT exposure and the release of ATP and HMGB-1 compared to other groups. Based on these results, combination therapy with DOX-BSA/MnO_2 and laser irradiation in a 4T1 tumor mouse model resulted in significantly enhanced therapeutic efficacy compared to other treatment groups. This outcome was further confirmed by increased M1 polarization, enhanced $CD8^+$ T cell infiltration, and decreased Treg levels in tumors extracted from the DOX-BSA/MnO_2 with the laser treatment group. The therapeutic potential was further validated through an abscopal model, demonstrating the effectiveness of the treatment.

Yun et al. developed silica-coated gold nanorods (AuNR@SiO_2) designed for mild-condition photothermal therapy (PTT) [118]. They identified the difficulty in achieving precise temperature control optimized for immunotherapy as a key limitation of traditional

PTT. To address this issue, they optimized the temperature by varying the thickness of the silica coating and treatment dosage of AuNR@SiO_2. Specifically, silica nanorods with a thickness of 20 nm (AuNR@SiO_2-20) demonstrated precise temperature control. When administered at different doses, 100 μg/kg of AuNR@SiO_2 induced a high proportion of early apoptosis, a condition favorable for active ICD. As a result, there was an enhanced release of DAMPs compared to the control group. When combined with PD-L1 antibodies, this approach achieved a 100% tumor clearance rate, demonstrating exceptional therapeutic efficacy. Furthermore, when cancer cells were re-inoculated into the cleared CT26 mouse models, tumor regression was observed in naive mice but not in the treated mouse models, indicating the acquisition of immune memory properties due to immune activation.

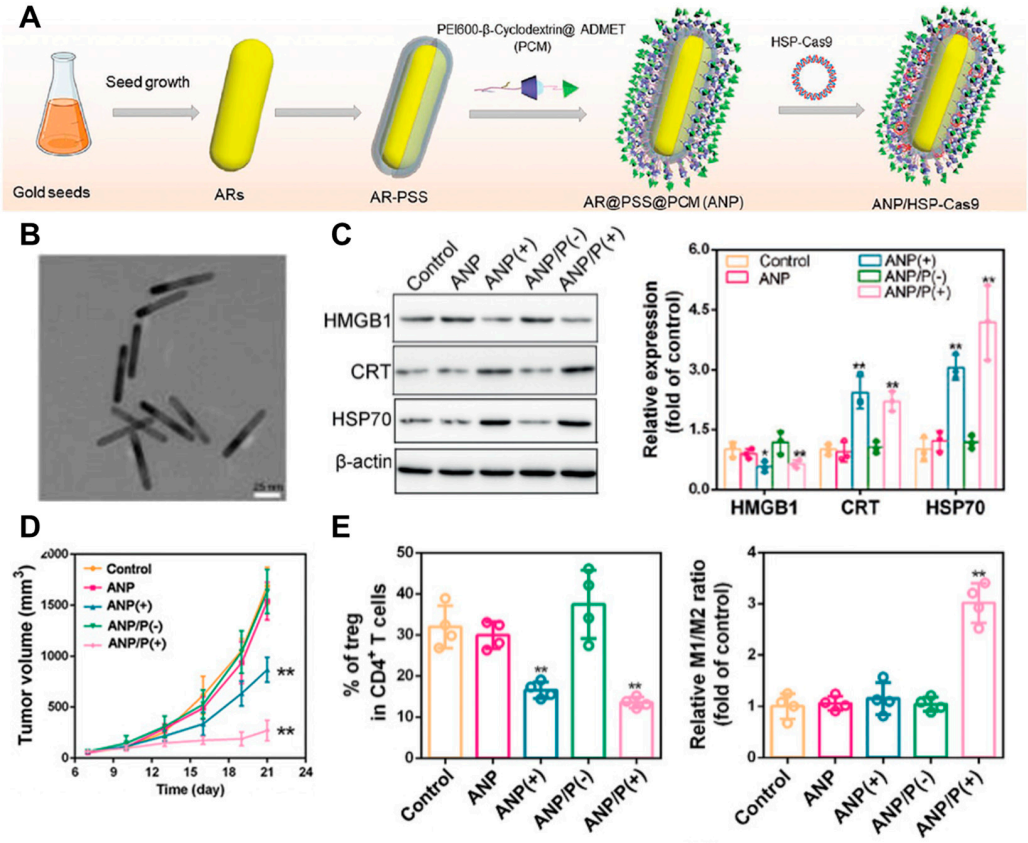


Figure 4. (**A**) Schematic illustration of ANP/HSP-Cas9 preparation. (**B**) TEM images of AR. (**C**) Western blot images of DAMPs (HMGB1, CRT, HSP70) after treatment and its quantification. (**D**) Tumor growth curve with the treatment of ANP, ANP with light, and ANP/P with or without light. (**E**) The relative expression level of Tregs and M1/M2 ratio at the tumor tissue. The significance was determined by Student's *t*-test (**C**,**E**) or one-way ANOVA using the Tukey post-test (**D**). (* $p < 0.05$, ** $p < 0.01$). Reproduced with permission. Copyright: Wiley-VCH GmbH, 2021.

6. Conclusions

As discussed earlier, the use of nanoparticles enables effective TME remodeling through the induction of ICD, facilitating complete tumor regression. The induction of ICD becomes more efficient and tumor-targeted by integrating nanoparticles with various treatments such as chemotherapy, PDT, radiation, and PTT. Furthermore, ongoing research aims to combine multiple therapeutic approaches, such as chemo-photodynamic therapy and chemo-radiation therapy, within a single nanoparticle platform. In the future, these advances are expected to lead to the development of a total solution, where a single nanoparticle carries customized therapeutic agents and methods tailored to individual patients. With continuous innovation and research, these technologies are anticipated to maximize the efficacy of PD-L1 antibodies in solid tumors and open new horizons in cancer treatment.

Author Contributions: S.H., J.P. and Y.O. contributed equally to this work. Investigation, S.H., J.P. and Y.O.; writing—original draft preparation, S.H. (Sections 1, 4 and 5), J.P. (Sections 1 and 3), Y.O. (Sections 1 and 2) and H.C. (Section 6, overall organization); writing—review and editing, K.K.; supervision, K.K.; funding acquisition, K.K. All authors have read and agreed to the published version of the manuscript.

Funding: This work was supported by a grant from the Korea Health Industry Development Institute (KHIDI), funded by the Ministry of Health and Welfare (HI23C0374), Republic of Korea.

Institutional Review Board Statement: Not applicable.

Informed Consent Statement: Not applicable.

Data Availability Statement: No new data were created or analyzed in this study.

Conflicts of Interest: The authors declare no conflicts of interest.

References

1. Wang, X.; Fan, S.; Pan, H.; Chen, W.; Wang, H. Cancer immunotherapy for metastasis: Past, present and future. *Brief. Funct. Genom.* **2019**, *18*, 140–146. [CrossRef] [PubMed]
2. Ribas, A.; Wolchok, J.D. Cancer immunotherapy using checkpoint blockade. *Science* **2018**, *359*, 1350–1355. [CrossRef] [PubMed]
3. Gupta, S.L.; Basu, S.; Soni, V.; Jaiswal, R.K. Immunotherapy: An alternative promising therapeutic approach against cancers. *Mol. Biol. Rep.* **2022**, *49*, 9903–9913. [CrossRef] [PubMed]
4. Yan, Y.; Kumar, A.B.; Finnes, H.; Markovic, S.N.; Park, S.; Dronca, R.S.; Dong, H. Combining Immune Checkpoint Inhibitors With Conventional Cancer Therapy. *Front. Immunol.* **2018**, *9*, 1739. [CrossRef]
5. Gotwals, P.; Cameron, S.; Cipolletta, D.; Cremasco, V.; Crystal, A.; Hewes, B.; Mueller, B.; Quaratino, S.; Sabatos-Peyton, C.; Petruzzelli, L.; et al. Prospects for combining targeted and conventional cancer therapy with immunotherapy. *Nat. Rev. Cancer* **2017**, *17*, 286–301. [CrossRef]
6. Rehammar, J.C.; Jensen, M.B.; McGale, P.; Lorenzen, E.L.; Taylor, C.; Darby, S.C.; Videbaek, L.; Wang, Z.; Ewertz, M. Risk of heart disease in relation to radiotherapy and chemotherapy with anthracyclines among 19,464 breast cancer patients in Denmark, 1977–2005. *Radiother. Oncol.* **2017**, *123*, 299–305. [CrossRef]
7. Monsuez, J.J.; Charniot, J.C.; Vignat, N.; Artigou, J.Y. Cardiac side-effects of cancer chemotherapy. *Int. J. Cardiol.* **2010**, *144*, 3–15. [CrossRef]
8. van den Boogaard, W.M.C.; Komninos, D.S.J.; Vermeij, W.P. Chemotherapy Side-Effects: Not All DNA Damage Is Equal. *Cancers* **2022**, *14*, 627. [CrossRef]
9. Feliu, J.; Jimenez-Munarriz, B.; Basterretxea, L.; Paredero, I.; Llabres, E.; Antonio-Rebollo, M.; Losada, B.; Espinosa, E.; Girones, R.; Custodio, A.B.; et al. Predicting Chemotherapy Toxicity in Older Patients with Cancer: A Multicenter Prospective Study. *Oncologist* **2020**, *25*, e1516–e1524. [CrossRef]
10. Buchbinder, E.I.; Desai, A. CTLA-4 and PD-1 Pathways: Similarities, Differences, and Implications of Their Inhibition. *Am. J. Clin. Oncol.* **2016**, *39*, 98–106. [CrossRef]
11. Ott, P.A.; Hodi, F.S.; Robert, C. CTLA-4 and PD-1/PD-L1 blockade: New immunotherapeutic modalities with durable clinical benefit in melanoma patients. *Clin. Cancer Res.* **2013**, *19*, 5300–5309. [CrossRef] [PubMed]
12. Wojtukiewicz, M.Z.; Rek, M.M.; Karpowicz, K.; Gorska, M.; Politynska, B.; Wojtukiewicz, A.M.; Moniuszko, M.; Radziwon, P.; Tucker, S.C.; Honn, K.V. Inhibitors of immune checkpoints-PD-1, PD-L1, CTLA-4-new opportunities for cancer patients and a new challenge for internists and general practitioners. *Cancer Metast. Rev.* **2021**, *40*, 949–982. [CrossRef] [PubMed]
13. Hargadon, K.M.; Johnson, C.E.; Williams, C.J. Immune checkpoint blockade therapy for cancer: An overview of FDA-approved immune checkpoint inhibitors. *Int. Immunopharmacol.* **2018**, *62*, 29–39. [CrossRef] [PubMed]
14. Gou, Q.; Dong, C.; Xu, H.; Khan, B.; Jin, J.; Liu, Q.; Shi, J.; Hou, Y. PD-L1 degradation pathway and immunotherapy for cancer. *Cell Death Dis.* **2020**, *11*, 955. [CrossRef]
15. Dobosz, P.; Stepien, M.; Golke, A.; Dzieciatkowski, T. Challenges of the Immunotherapy: Perspectives and Limitations of the Immune Checkpoint Inhibitor Treatment. *Int. J. Mol. Sci.* **2022**, *23*, 2847. [CrossRef]
16. Gupta, S.; Shukla, S. Limitations of Immunotherapy in Cancer. *Cureus* **2022**, *14*, e30856. [CrossRef]
17. Liu, C.; Yang, M.; Zhang, D.; Chen, M.; Zhu, D. Clinical cancer immunotherapy: Current progress and prospects. *Front. Immunol.* **2022**, *13*, 961805. [CrossRef]
18. Meng, J.; Lu, X.; Zhou, Y.; Zhang, M.; Ge, Q.; Zhou, J.; Hao, Z.; Gao, S.; Yan, F.; Liang, C. Tumor immune microenvironment-based classifications of bladder cancer for enhancing the response rate of immunotherapy. *Mol. Ther.-Oncolyt.* **2021**, *20*, 410–421. [CrossRef]
19. Tang, L.; Huang, Z.; Mei, H.; Hu, Y. Immunotherapy in hematologic malignancies: Achievements, challenges and future prospects. *Signal Transduct. Target. Ther.* **2023**, *8*, 306. [CrossRef]
20. Marciscano, A.E.; Anandasabapathy, N. The role of dendritic cells in cancer and anti-tumor immunity. *Semin. Immunol.* **2021**, *52*, 101481. [CrossRef]

21. Gardner, A.; Ruffell, B. Dendritic Cells and Cancer Immunity. *Trends Immunol.* **2016**, *37*, 855–865. [CrossRef] [PubMed]
22. Zhu, Y.; Yu, X.; Thamphiwatana, S.D.; Zheng, Y.; Pang, Z. Nanomedicines modulating tumor immunosuppressive cells to enhance cancer immunotherapy. *Acta Pharm. Sin. B* **2020**, *10*, 2054–2074. [CrossRef] [PubMed]
23. Yang, L.; Li, A.; Lei, Q.; Zhang, Y. Tumor-intrinsic signaling pathways: Key roles in the regulation of the immunosuppressive tumor microenvironment. *J. Hematol. Oncol.* **2019**, *12*, 125. [CrossRef] [PubMed]
24. Li, X.; Guo, X.; Ling, J.; Tang, Z.; Huang, G.; He, L.; Chen, T. Nanomedicine-based cancer immunotherapies developed by reprogramming tumor-associated macrophages. *Nanoscale* **2021**, *13*, 4705–4727. [CrossRef]
25. Liu, J.; Bai, Y.; Li, Y.; Li, X.; Luo, K. Reprogramming the immunosuppressive tumor microenvironment through nanomedicine: An immunometabolism perspective. *EBioMedicine* **2024**, *107*, 105301. [CrossRef]
26. Li, Z.; Lai, X.; Fu, S.; Ren, L.; Cai, H.; Zhang, H.; Gu, Z.; Ma, X.; Luo, K. Immunogenic Cell Death Activates the Tumor Immune Microenvironment to Boost the Immunotherapy Efficiency. *Adv. Sci.* **2022**, *9*, e2201734. [CrossRef]
27. Yang, W.; Yi, J.; Zhu, R.; Guo, Y.; Zhang, K.; Cao, Y.; Li, X.; Zhang, J.; Zhang, Z.; Li, Y.; et al. Transformable prodrug nanoplatform via tumor microenvironment modulation and immune checkpoint blockade potentiates immunogenic cell death mediated cancer immunotherapy. *Theranostics* **2023**, *13*, 1906–1920. [CrossRef]
28. Nicoletto, R.E.; Ofner, C.M., 3rd. Cytotoxic mechanisms of doxorubicin at clinically relevant concentrations in breast cancer cells. *Cancer Chemother. Pharmacol.* **2022**, *89*, 285–311. [CrossRef]
29. Thorn, C.F.; Oshiro, C.; Marsh, S.; Hernandez-Boussard, T.; McLeod, H.; Klein, T.E.; Altman, R.B. Doxorubicin pathways: Pharmacodynamics and adverse effects. *Pharmacogenet. Genom.* **2011**, *21*, 440–446. [CrossRef]
30. Murao, A.; Aziz, M.; Wang, H.; Brenner, M.; Wang, P. Release mechanisms of major DAMPs. *Apoptosis* **2021**, *26*, 152–162. [CrossRef]
31. Parker, K.H.; Sinha, P.; Horn, L.A.; Clements, V.K.; Yang, H.; Li, J.; Tracey, K.J.; Ostrand-Rosenberg, S. HMGB1 enhances immune suppression by facilitating the differentiation and suppressive activity of myeloid-derived suppressor cells. *Cancer Res.* **2014**, *74*, 5723–5733. [CrossRef] [PubMed]
32. Hou, G.; Chen, Y.; Lei, H.; Lu, Y.; Liu, L.; Han, Z.; Sun, S.; Li, J.; Cheng, L. Bimetallic peroxide nanoparticles induce PANoptosis by disrupting ion homeostasis for enhanced immunotherapy. *Sci. Adv.* **2024**, *10*, eadp7160. [CrossRef] [PubMed]
33. Liu, L.; Peng, S.; Duan, M.; Liu, C.; Li, L.; Zhang, X.; Ren, B.; Tian, H. The role of C/EBP homologous protein (CHOP) in regulating macrophage polarization in RAW264.7 cells. *Microbiol. Immunol.* **2021**, *65*, 531–541. [CrossRef] [PubMed]
34. Dosch, M.; Gerber, J.; Jebbawi, F.; Beldi, G. Mechanisms of ATP Release by Inflammatory Cells. *Int. J. Mol. Sci.* **2018**, *19*, 1222. [CrossRef]
35. Wang, Y.; Xiang, Y.; Xin, V.W.; Wang, X.W.; Peng, X.C.; Liu, X.Q.; Wang, D.; Li, N.; Cheng, J.T.; Lyv, Y.N.; et al. Dendritic cell biology and its role in tumor immunotherapy. *J. Hematol. Oncol.* **2020**, *13*, 107. [CrossRef]
36. Wang, B.; Han, Y.; Zhang, Y.; Zhao, Q.; Wang, H.; Wei, J.; Meng, L.; Xin, Y.; Jiang, X. Overcoming acquired resistance to cancer immune checkpoint therapy: Potential strategies based on molecular mechanisms. *Cell Biosci.* **2023**, *13*, 120. [CrossRef]
37. Marei, H.E.; Hasan, A.; Pozzoli, G.; Cenciarelli, C. Cancer immunotherapy with immune checkpoint inhibitors (ICIs): Potential, mechanisms of resistance, and strategies for reinvigorating T cell responsiveness when resistance is acquired. *Cancer Cell Int.* **2023**, *23*, 64. [CrossRef]
38. Li, W.; Jiang, Y.; Lu, J. Nanotechnology-enabled immunogenic cell death for improved cancer immunotherapy. *Int. J. Pharm.* **2023**, *634*, 122655. [CrossRef]
39. Li, Y.; Liu, X.; Zhang, X.; Pan, W.; Li, N.; Tang, B. Immunogenic cell death inducers for enhanced cancer immunotherapy. *Chem. Commun.* **2021**, *57*, 12087–12097. [CrossRef]
40. Xie, D.; Wang, Q.; Wu, G. Research progress in inducing immunogenic cell death of tumor cells. *Front. Immunol.* **2022**, *13*, 1017400. [CrossRef]
41. Bahreyni, A.; Mohamud, Y.; Zhang, J.; Luo, H. Engineering a facile and versatile nanoplatform to facilitate the delivery of multiple agents for targeted breast cancer chemo-immunotherapy. *Biomed. Pharmacother.* **2023**, *163*, 114789. [CrossRef] [PubMed]
42. Chen, Q.; Li, C.; Wang, Q. Multifunctional Nano-Biomaterials for Cancer Therapy via Inducing Enhanced Immunogenic Cell Death. *Small Methods* **2023**, *7*, e2201457. [CrossRef] [PubMed]
43. Shim, G.; Jeong, S.; Oh, J.L.; Kang, Y. Lipid-based nanoparticles for photosensitive drug delivery systems. *J. Pharm. Investig.* **2022**, *52*, 151–160. [CrossRef] [PubMed]
44. Shim, N.; Cho, H.H.; Jeon, S.I.; Kim, K. Recent developments in chemodrug-loaded nanomedicines and their application in combination cancer immunotherapy. *J. Pharm. Investig.* **2024**, *54*, 13–36. [CrossRef]
45. Zeb, A.; Gul, M.; Nguyen, T.T.L.; Maeng, H.J. Controlled release and targeted drug delivery with poly(lactic-co-glycolic acid) nanoparticles: Reviewing two decades of research. *J. Pharm. Investig.* **2022**, *52*, 683–724. [CrossRef]
46. Shrestha, S.; Shrestha, A.; Kim, J.; Thapa, R.K.; Kim, J.O. Recent advances in albumin nanoparticle-based cancer therapies. *J. Pharm. Investig.* **2024**. [CrossRef]
47. Zeb, A.; Gul, M.; Nguyen, T.T.L.; Maeng, H.J. Recent progress and drug delivery applications of surface-functionalized inorganic nanoparticles in cancer therapy. *J. Pharm. Investig.* **2023**, *53*, 743–779. [CrossRef]
48. Karmacharya, P.; Patil, B.R.; Kim, J.O. Recent advancements in lipid-mRNA nanoparticles as a treatment option for cancer immunotherapy. *J. Pharm. Investig.* **2022**, *52*, 415–426. [CrossRef]

49. Subbaraj, G.K.; Masoodi, T.; Yasam, S.K.; Chandrashekar, K.; Kulanthaivel, L.; Shaik, N.A.; Hashem, S.; Alshabeeb Akil, A.S.; Bhat, A.A. Anti-angiogenic effect of nano-formulated water soluble kaempferol and combretastatin in an in vivo chick chorioallantoic membrane model and HUVEC cells. *Biomed. Pharmacother.* **2023**, *163*, 114820. [CrossRef]
50. Majima, M.; Hosono, K.; Ito, Y.; Amano, H.; Nagashima, Y.; Matsuda, Y.; Watanabe, S.I.; Nishimura, H. A biologically active lipid, thromboxane, as a regulator of angiogenesis and lymphangiogenesis. *Biomed. Pharmacother.* **2023**, *163*, 114831. [CrossRef]
51. Priya, S.; Desai, V.M.; Singhvi, G. Surface Modification of Lipid-Based Nanocarriers: A Potential Approach to Enhance Targeted Drug Delivery. *ACS Omega* **2023**, *8*, 74–86. [CrossRef] [PubMed]
52. Hong, L.; Li, W.; Li, Y.; Yin, S. Nanoparticle-based drug delivery systems targeting cancer cell surfaces. *RSC Adv.* **2023**, *13*, 21365–21382. [CrossRef] [PubMed]
53. Wu, P.; Han, J.; Gong, Y.; Liu, C.; Yu, H.; Xie, N. Nanoparticle-Based Drug Delivery Systems Targeting Tumor Microenvironment for Cancer Immunotherapy Resistance: Current Advances and Applications. *Pharmaceutics* **2022**, *14*, 1990. [CrossRef] [PubMed]
54. Cheng, F.; He, L.; Wang, J.; Lai, L.; Ma, L.; Qu, K.; Yang, Z.; Wang, X.; Zhao, R.; Weng, L.; et al. Synergistic immunotherapy with a calcium-based nanoinducer: Evoking pyroptosis and remodeling tumor-associated macrophages for enhanced antitumor immune response. *Nanoscale* **2024**, *16*, 18570–18583. [CrossRef]
55. Tian, M.; Liu, X.; Pei, H. Nanomaterial-based cancer immunotherapy: Enhancing treatment strategies. *Front. Chem.* **2024**, *12*, 1492215. [CrossRef]
56. Lu, Q.; Kou, D.; Lou, S.; Ashrafizadeh, M.; Aref, A.R.; Canadas, I.; Tian, Y.; Niu, X.; Wang, Y.; Torabian, P.; et al. Nanoparticles in tumor microenvironment remodeling and cancer immunotherapy. *J. Hematol. Oncol.* **2024**, *17*, 16. [CrossRef]
57. He, M.; Zhang, M.; Xu, T.; Xue, S.; Li, D.; Zhao, Y.; Zhi, F.; Ding, D. Enhancing photodynamic immunotherapy by reprograming the immunosuppressive tumor microenvironment with hypoxia relief. *J. Control. Release* **2024**, *368*, 233–250. [CrossRef]
58. Gao, S.; Yang, D.; Fang, Y.; Lin, X.; Jin, X.; Wang, Q.; Wang, X.; Ke, L.; Shi, K. Engineering Nanoparticles for Targeted Remodeling of the Tumor Microenvironment to Improve Cancer Immunotherapy. *Theranostics* **2019**, *9*, 126–151. [CrossRef]
59. Cheng, Z.; Fobian, S.F.; Gurrieri, E.; Amin, M.; D'Agostino, V.G.; Falahati, M.; Zalba, S.; Debets, R.; Garrido, M.J.; Saeed, M.; et al. Lipid-based nanosystems: The next generation of cancer immune therapy. *J. Hematol. Oncol.* **2024**, *17*, 53. [CrossRef]
60. Huang, X.; Ren, Q.; Yang, L.; Cui, D.; Ma, C.; Zheng, Y.; Wu, J. Immunogenic chemotherapy: Great potential for improving response rates. *Front. Oncol.* **2023**, *13*, 1308681. [CrossRef]
61. Huang, T.; Sun, X.; Qi, Y.; Yang, X.; Fan, L.; Chen, M.; Yue, Y.; Ge, H.; Li, Y.; Nie, G.; et al. Immunogenic cell death effects induced by doxorubicin improved chemo-immunotherapy via restoration of granzyme B activity. *Nano Res.* **2023**, *16*, 13250–13258. [CrossRef]
62. Rozpedek, W.; Pytel, D.; Mucha, B.; Leszczynska, H.; Diehl, J.A.; Majsterek, I. The Role of the PERK/eIF2alpha/ATF4/CHOP Signaling Pathway in Tumor Progression During Endoplasmic Reticulum Stress. *Curr. Mol. Med.* **2016**, *16*, 533–544. [CrossRef] [PubMed]
63. Correia de Sousa, M.; Delangre, E.; Turkal, M.; Foti, M.; Gjorgjieva, M. Endoplasmic Reticulum Stress in Renal Cell Carcinoma. *Int. J. Mol. Sci.* **2023**, *24*, 4914. [CrossRef] [PubMed]
64. Fu, X.; Cui, J.; Meng, X.; Jiang, P.; Zheng, Q.; Zhao, W.; Chen, X. Endoplasmic reticulum stress, cell death and tumor: Association between endoplasmic reticulum stress and the apoptosis pathway in tumors (Review). *Oncol. Rep.* **2021**, *45*, 801–808. [CrossRef] [PubMed]
65. Sprooten, J.; Laureano, R.S.; Vanmeerbeek, I.; Govaerts, J.; Naulaerts, S.; Borras, D.M.; Kinget, L.; Fucikova, J.; Spisek, R.; Jelinkova, L.P.; et al. Trial watch: Chemotherapy-induced immunogenic cell death in oncology. *Oncoimmunology* **2023**, *12*, 2219591. [CrossRef]
66. Wang, J.; Ma, J.; Xie, F.; Miao, F.; Lv, L.; Huang, Y.; Zhang, X.; Yu, J.; Tai, Z.; Zhu, Q.; et al. Immunogenic cell death-based cancer vaccines: Promising prospect in cancer therapy. *Front. Immunol.* **2024**, *15*, 1389173. [CrossRef]
67. Jiang, M.; Zeng, J.; Zhao, L.; Zhang, M.; Ma, J.; Guan, X.; Zhang, W. Chemotherapeutic drug-induced immunogenic cell death for nanomedicine-based cancer chemo-immunotherapy. *Nanoscale* **2021**, *13*, 17218–17235. [CrossRef]
68. Kim, J.; Shim, M.K.; Moon, Y.; Kim, J.; Cho, H.; Yun, W.S.; Shim, N.; Seong, J.K.; Lee, Y.; Lim, D.K.; et al. Cancer cell-specific and pro-apoptotic SMAC peptide-doxorubicin conjugated prodrug encapsulated aposomes for synergistic cancer immunotherapy. *J. Nanobiotechnol.* **2024**, *22*, 109. [CrossRef]
69. Yang, Q.; Shi, G.; Chen, X.; Lin, Y.; Cheng, L.; Jiang, Q.; Yan, X.; Jiang, M.; Li, Y.; Zhang, H.; et al. Nanomicelle protects the immune activation effects of Paclitaxel and sensitizes tumors to anti-PD-1 Immunotherapy. *Theranostics* **2020**, *10*, 8382–8399. [CrossRef]
70. Zhang, N.; Li, J.; Gao, W.; Zhu, W.; Yan, J.; He, Z.; Li, L.; Wu, F.; Pu, Y.; He, B. Co-Delivery of Doxorubicin and Anti-PD-L1 Peptide in Lipid/PLGA Nanocomplexes for the Chemo-Immunotherapy of Cancer. *Mol. Pharm.* **2022**, *19*, 3439–3449. [CrossRef]
71. Song, S.; Shim, M.K.; Yang, S.; Lee, J.; Yun, W.S.; Cho, H.; Moon, Y.; Min, J.Y.; Han, E.H.; Yoon, H.Y.; et al. All-in-one glycol chitosan nanoparticles for co-delivery of doxorubicin and anti-PD-L1 peptide in cancer immunotherapy. *Bioact. Mater.* **2023**, *28*, 358–375. [CrossRef] [PubMed]
72. Alzeibak, R.; Mishchenko, T.A.; Shilyagina, N.Y.; Balalaeva, I.V.; Vedunova, M.V.; Krysko, D.V. Targeting immunogenic cancer cell death by photodynamic therapy: Past, present and future. *J. Immunother. Cancer* **2021**, *9*, e001926. [CrossRef] [PubMed]
73. Turubanova, V.D.; Balalaeva, I.V.; Mishchenko, T.A.; Catanzaro, E.; Alzeibak, R.; Peskova, N.N.; Efimova, I.; Bachert, C.; Mitroshina, E.V.; Krysko, O.; et al. Immunogenic cell death induced by a new photodynamic therapy based on photosens and photodithazine. *J. Immunother. Cancer* **2019**, *7*, 350. [CrossRef] [PubMed]

74. Correia, J.H.; Rodrigues, J.A.; Pimenta, S.; Dong, T.; Yang, Z. Photodynamic Therapy Review: Principles, Photosensitizers, Applications, and Future Directions. *Pharmaceutics* **2021**, *13*, 1332. [CrossRef]
75. Przygoda, M.; Bartusik-Aebisher, D.; Dynarowicz, K.; Cieslar, G.; Kawczyk-Krupka, A.; Aebisher, D. Cellular Mechanisms of Singlet Oxygen in Photodynamic Therapy. *Int. J. Mol. Sci.* **2023**, *24*, 16890. [CrossRef]
76. Zhou, Z.; Song, J.; Nie, L.; Chen, X. Reactive oxygen species generating systems meeting challenges of photodynamic cancer therapy. *Chem. Soc. Rev.* **2016**, *45*, 6597–6626. [CrossRef]
77. Castano, A.P.; Demidova, T.N.; Hamblin, M.R. Mechanisms in photodynamic therapy: Part one-photosensitizers, photochemistry and cellular localization. *Photodiagn. Photodyn. Ther.* **2004**, *1*, 279–293. [CrossRef]
78. Deng, H.; Zhou, Z.; Yang, W.; Lin, L.S.; Wang, S.; Niu, G.; Song, J.; Chen, X. Endoplasmic Reticulum Targeting to Amplify Immunogenic Cell Death for Cancer Immunotherapy. *Nano Lett.* **2020**, *20*, 1928–1933. [CrossRef]
79. Li, W.; Yang, J.; Luo, L.; Jiang, M.; Qin, B.; Yin, H.; Zhu, C.; Yuan, X.; Zhang, J.; Luo, Z.; et al. Targeting photodynamic and photothermal therapy to the endoplasmic reticulum enhances immunogenic cancer cell death. *Nat. Commun.* **2019**, *10*, 3349. [CrossRef]
80. Zheng, Y.; Yin, G.; Le, V.; Zhang, A.; Chen, S.; Liang, X.; Liu, J. Photodynamic-therapy Activates Immune Response by disrupting Immunity Homeostasis of Tumor Cells, which Generates Vaccine for Cancer Therapy. *Int. J. Biol. Sci.* **2016**, *12*, 120–132. [CrossRef]
81. Mroz, P.; Hashmi, J.T.; Huang, Y.Y.; Lange, N.; Hamblin, M.R. Stimulation of anti-tumor immunity by photodynamic therapy. *Expert. Rev. Clin. Immunol.* **2011**, *7*, 75–91. [CrossRef] [PubMed]
82. Chen, F.; Tang, H.; Cai, X.; Lin, J.; Kang, R.; Tang, D.; Liu, J. DAMPs in immunosenescence and cancer. *Semin. Cancer Biol.* **2024**, *106–107*, 123–142. [CrossRef] [PubMed]
83. Choi, J.; Park, B.; Park, J.Y.; Shin, D.; Lee, S.; Yoon, H.Y.; Kim, K.; Kim, S.H.; Kim, Y.; Yang, Y.; et al. Light-Triggered PROTAC Nanoassemblies for Photodynamic IDO Proteolysis in Cancer Immunotherapy. *Adv. Mater.* **2024**, *36*, e2405475. [CrossRef] [PubMed]
84. Wang, H.; Wang, K.; He, L.; Liu, Y.; Dong, H.; Li, Y. Engineering antigen as photosensitiser nanocarrier to facilitate ROS triggered immune cascade for photodynamic immunotherapy. *Biomaterials* **2020**, *244*, 119964. [CrossRef]
85. Zhao, H.; Xu, J.; Wang, Y.; Sun, C.; Bao, L.; Zhao, Y.; Yang, X.; Zhao, Y. A Photosensitizer Discretely Loaded Nanoaggregate with Robust Photodynamic Effect for Local Treatment Triggers Systemic Antitumor Responses. *ACS Nano* **2022**, *16*, 3070–3080. [CrossRef]
86. Jin, F.; Qi, J.; Liu, D.; You, Y.; Shu, G.; Du, Y.; Wang, J.; Xu, X.; Ying, X.; Ji, J.; et al. Cancer-cell-biomimetic Upconversion nanoparticles combining chemo-photodynamic therapy and CD73 blockade for metastatic triple-negative breast cancer. *J. Control. Release* **2021**, *337*, 90–104. [CrossRef]
87. Zhu, S.; Wang, Y.; Tang, J.; Cao, M. Radiotherapy induced immunogenic cell death by remodeling tumor immune microenvironment. *Front. Immunol.* **2022**, *13*, 1074477. [CrossRef]
88. Wang, J.S.; Wang, H.J.; Qian, H.L. Biological effects of radiation on cancer cells. *Mil. Med. Res.* **2018**, *5*, 20. [CrossRef]
89. Storozynsky, Q.; Hitt, M.M. The Impact of Radiation-Induced DNA Damage on cGAS-STING-Mediated Immune Responses to Cancer. *Int. J. Mol. Sci.* **2020**, *21*, 8877. [CrossRef]
90. Biau, J.; Chautard, E.; Verrelle, P.; Dutreix, M. Altering DNA Repair to Improve Radiation Therapy: Specific and Multiple Pathway Targeting. *Front. Oncol.* **2019**, *9*, 1009. [CrossRef]
91. Huang, R.X.; Zhou, P.K. DNA damage response signaling pathways and targets for radiotherapy sensitization in cancer. *Signal Transduct. Target. Ther.* **2020**, *5*, 60. [CrossRef] [PubMed]
92. Zhu, M.; Yang, M.; Zhang, J.; Yin, Y.; Fan, X.; Zhang, Y.; Qin, S.; Zhang, H.; Yu, F. Immunogenic Cell Death Induction by Ionizing Radiation. *Front. Immunol.* **2021**, *12*, 705361. [CrossRef] [PubMed]
93. Golden, E.B.; Apetoh, L. Radiotherapy and immunogenic cell death. *Semin. Radiat. Oncol.* **2015**, *25*, 11–17. [CrossRef] [PubMed]
94. Vaes, R.D.W.; Hendriks, L.E.L.; Vooijs, M.; De Ruysscher, D. Biomarkers of Radiotherapy-Induced Immunogenic Cell Death. *Cells* **2021**, *10*, 930. [CrossRef]
95. Kang, J.; Demaria, S.; Formenti, S. Current clinical trials testing the combination of immunotherapy with radiotherapy. *J. Immunother. Cancer* **2016**, *4*, 51. [CrossRef]
96. Yu, S.; Wang, Y.; He, P.; Shao, B.; Liu, F.; Xiang, Z.; Yang, T.; Zeng, Y.; He, T.; Ma, J.; et al. Effective Combinations of Immunotherapy and Radiotherapy for Cancer Treatment. *Front. Oncol.* **2022**, *12*, 809304. [CrossRef]
97. Zhang, Z.; Liu, X.; Chen, D.; Yu, J. Radiotherapy combined with immunotherapy: The dawn of cancer treatment. *Signal Transduct. Target. Ther.* **2022**, *7*, 258. [CrossRef]
98. Chen, Q.; Chen, J.; Yang, Z.; Xu, J.; Xu, L.; Liang, C.; Han, X.; Liu, Z. Nanoparticle-Enhanced Radiotherapy to Trigger Robust Cancer Immunotherapy. *Adv. Mater.* **2019**, *31*, e1802228. [CrossRef]
99. Wang, Y.; Wang, L.; Li, T.; Ouyang, M.; Xiong, H.; Zhou, D. Bimetallic nanoparticles as cascade sensitizing amplifiers for low-dose and robust cancer radio-immunotherapy. *Acta Pharm. Sin. B* **2024**, *14*, 1787–1800. [CrossRef]
100. Huang, Z.; Wang, Y.; Yao, D.; Wu, J.; Hu, Y.; Yuan, A. Nanoscale coordination polymers induce immunogenic cell death by amplifying radiation therapy mediated oxidative stress. *Nat. Commun.* **2021**, *12*, 145. [CrossRef]
101. Guan, X.; Sun, L.; Shen, Y.; Jin, F.; Bo, X.; Zhu, C.; Han, X.; Li, X.; Chen, Y.; Xu, H.; et al. Nanoparticle-enhanced radiotherapy synergizes with PD-L1 blockade to limit post-surgical cancer recurrence and metastasis. *Nat. Commun.* **2022**, *13*, 2834. [CrossRef] [PubMed]

102. Zeng, W.; Li, Z.; Chen, H.; Zeng, X.; Mei, L. An optimal portfolio of photothermal combined immunotherapy. *Cell Rep. Phys. Sci.* **2022**, *3*, 100898. [CrossRef]
103. Sun, H.; Zhang, Q.; Li, J.; Peng, S.; Wang, X.; Cai, R. Near-infrared photoactivated nanomedicines for photothermal synergistic cancer therapy. *Nano Today* **2021**, *37*, 101073. [CrossRef]
104. Bao, X.; Yuan, Y.; Chen, J.; Zhang, B.; Li, D.; Zhou, D.; Jing, P.; Xu, G.; Wang, Y.; Hola, K.; et al. In vivo theranostics with near-infrared-emitting carbon dots-highly efficient photothermal therapy based on passive targeting after intravenous administration. *Light Sci. Appl.* **2018**, *7*, 91. [CrossRef]
105. Gai, L.X.; Wang, W.Q.; Wu, X.; Su, X.J.; Yang, F.C. NIR absorbing reduced graphene oxide for photothermal radiotherapy for treatment of esophageal cancer. *J. Photochem. Photobiol. B* **2019**, *194*, 188–193. [CrossRef]
106. Yu, S.; Xia, G.; Yang, N.; Yuan, L.; Li, J.; Wang, Q.; Li, D.; Ding, L.; Fan, Z.; Li, J. Noble Metal Nanoparticle-Based Photothermal Therapy: Development and Application in Effective Cancer Therapy. *Int. J. Mol. Sci.* **2024**, *25*, 5632. [CrossRef]
107. Naskar, A.; Kim, K.S. Friends against the Foe: Synergistic Photothermal and Photodynamic Therapy against Bacterial Infections. *Pharmaceutics* **2023**, *15*, 1116. [CrossRef]
108. Indhu, A.R.; Keerthana, L.; Dharmalingam, G. Plasmonic nanotechnology for photothermal applications—An evaluation. *Beilstein J. Nanotechnol.* **2023**, *14*, 380–419. [CrossRef]
109. Li, J.; Zhang, W.; Ji, W.; Wang, J.; Wang, N.; Wu, W.; Wu, Q.; Hou, X.; Hu, W.; Li, L. Near infrared photothermal conversion materials: Mechanism, preparation, and photothermal cancer therapy applications. *J. Mater. Chem. B* **2021**, *9*, 7909–7926. [CrossRef]
110. Kim, M.; Lee, J.H.; Nam, J.M. Plasmonic Photothermal Nanoparticles for Biomedical Applications. *Adv. Sci.* **2019**, *6*, 1900471. [CrossRef]
111. Xie, M.; Gong, T.; Wang, Y.; Li, Z.; Lu, M.; Luo, Y.; Min, L.; Tu, C.; Zhang, X.; Zeng, Q.; et al. Advancements in Photothermal Therapy Using Near-Infrared Light for Bone Tumors. *Int. J. Mol. Sci.* **2024**, *25*, 4139. [CrossRef] [PubMed]
112. Guo, R.; Wang, S.; Zhao, L.; Zong, Q.; Li, T.; Ling, G.; Zhang, P. Engineered nanomaterials for synergistic photo-immunotherapy. *Biomaterials* **2022**, *282*, 121425. [CrossRef] [PubMed]
113. Xu, P.; Liang, F. Nanomaterial-Based Tumor Photothermal Immunotherapy. *Int. J. Nanomed.* **2020**, *15*, 9159–9180. [CrossRef] [PubMed]
114. Huang, X.; Lu, Y.; Guo, M.; Du, S.; Han, N. Recent strategies for nano-based PTT combined with immunotherapy: From a biomaterial point of view. *Theranostics* **2021**, *11*, 7546–7569. [CrossRef]
115. Chen, W.; Qin, M.; Chen, X.; Wang, Q.; Zhang, Z.; Sun, X. Combining photothermal therapy and immunotherapy against melanoma by polydopamine-coated Al_2O_3 nanoparticles. *Theranostics* **2018**, *8*, 2229–2241. [CrossRef]
116. Tang, H.; Xu, X.; Chen, Y.; Xin, H.; Wan, T.; Li, B.; Pan, H.; Li, D.; Ping, Y. Reprogramming the Tumor Microenvironment through Second-Near-Infrared-Window Photothermal Genome Editing of *PD-L1* Mediated by Supramolecular Gold Nanorods for Enhanced Cancer Immunotherapy. *Adv. Mater.* **2021**, *33*, 2006003. [CrossRef]
117. Chen, Z.; Zhang, Q.; Huang, Q.; Liu, Z.; Zeng, L.; Zhang, L.; Chen, X.; Song, H.; Zhang, J. Photothermal MnO_2 nanoparticles boost chemo-photothermal therapy-induced immunogenic cell death in tumor immunotherapy. *Int. J. Pharm.* **2022**, *617*, 121578. [CrossRef]
118. Yun, W.S.; Yang, W.; Shim, M.K.; Song, S.; Choi, J.; Kim, J.; Kim, J.; Moon, Y.; Jo, S.; Lim, D.K.; et al. Accurately Controlled Tumor Temperature with Silica-Coated Gold Nanorods for Optimal Immune Checkpoint Blockade Therapy. *Biomater. Res.* **2024**, *28*, 0024. [CrossRef]

Disclaimer/Publisher's Note: The statements, opinions and data contained in all publications are solely those of the individual author(s) and contributor(s) and not of MDPI and/or the editor(s). MDPI and/or the editor(s) disclaim responsibility for any injury to people or property resulting from any ideas, methods, instructions or products referred to in the content.